IEEE Access
Multidisciplinary | Rapid Review | Open Access Journal

Received October 20, 2020, accepted November 4, 2020, date of publication November 9, 2020, date of current version November 24, 2020.

Digital Object Identifier 10.1109/ACCESS.2020.3036840

Prediction of Pollution State of Heating Surface in Coal-Fired Utility Boilers

QIANG LI[1], PEIGANG YAN[1], JINFU LIU[1], YUANHAO SHI[2], AND DAREN YU[1]
[1]School of Energy Science and Engineering, Harbin Institute of Technology, Harbin 150001, China
[2]School of Electrical and Control Engineering, North University of China, Taiyuan 030051, China

Corresponding author: Jinfu Liu (jinfuliuhit@163.com)

This work was supported by the National Key Research and Development Program of China under Grant 2017YFB0902100.

ABSTRACT This paper presents a method to predict the cleaning state of the boiler heating surface. In this method, firstly, the historical fouling rate data is decomposed into two parts: fitting curve data and the difference between original data and the fitting curve. Then, combined with the real-time fouling rate data, the prediction model is established. Finally, the method is verified by the actual operation data of a 300 MW coal-fired power station boiler. The method does not need additional special instruments or a complex calculation system but can use the existing monitoring data to realize the dirt monitoring and soot blowing optimization of the economizer, which has a certain guiding role for the soot blowing operation of the coal-fired power plant.

INDEX TERMS Boiler heating surface, fouling rate, fitting, difference, prediction.

I. INTRODUCTION

Although renewable energy power plants (wind, solar, hydro, geothermal, tidal, etc.) have experienced strong development in the past 10 years, fossil fuel power plants are still the main power supply source in many countries. According to the International Energy Agency, 75% of energy will still be supplied by fossil fuels by 2030 [1]. At present, coal is the main power generation form of fossil fuel power plants. The boiler is the key equipment of power plant operation. In the process of coal-fired boiler operation, there will inevitably be different degrees of ash (slagging and ash deposition) on each heating surface. According to the survey conducted by the American Electric Power Research Institute(EPRI) on the ash pollution of 91 power station boilers in the United States, the statistical data show that 37% of the boiler units frequently suffer from serious ash pollution, and 40% of the boiler units occasionally suffer from ash pollution [2]. Slagging and ash deposition on the heating surface have many adverse effects on the economic and safe operation of coal-fired units [3]–[5], mainly reflected in the following aspects: first, it affects the heat transfer efficiency of the heating surface. Second, slagging and ash deposition will inevitably cause corrosion and wear of the metal on the heating surface. Finally, if there is too much ash and it is not removed in time and effectively, it will block the flue, increase the ventilation resistance, and reduce the boiler output. Due to the high-temperature corrosion of the pipe wall, the local temperature of the pipe wall is too high and the pipe wall is worn, which may cause the explosion accident and endanger the safety production.

In the process of boiler operation, the use of soot blowers can effectively avoid serious ash deposition and slagging on the heating surface. At present, advanced soot blowing equipment has been installed in large-scale coal-fired power plants, and the problem of low operation rate of soot blower has been solved. Conventional soot blowing methods include steam soot blowing, acoustic soot blowing, gas pulse soot blowing, and so on, among which steam soot blowing is the most widely used. At present, the soot blowing operation of each heating surface of the coal-fired power plant is mainly based on the fixed daily operation mode and the daily operation time. The change of coal type and boiler operation condition will affect the ash deposition speed of the heating surface. The constant regular soot blowing is not in line with the actual situation of operation. If the soot blowing operation is not carried out in time, it will cause too much ash deposition on the heating surface, reduce the heat transfer efficiency, and even cause accidents, which will affect the safety and economy of boiler production; if the soot blowing frequency is too high,

The associate editor coordinating the review of this manuscript and approving it for publication was Xiao-Sheng Si.

This work is licensed under a Creative Commons Attribution-NonCommercial-NoDerivatives 4.0 License.
For more information, see https://creativecommons.org/licenses/by-nc-nd/4.0/

it will not only cause excessive waste of soot blowing steam, but also cause erosion of heating surface and affect the service life of equipment. Therefore, under the limited conditions of soot blowing cost, production efficiency, and production constraints, it is of great significance to determine the most efficient soot blowing operation mode for the safety of the whole unit, energy saving and emission reduction [6]–[9].

In recent years, many scholars have done a lot of research on soot monitoring and soot blowing optimization of the heating surface of coal-fired power plant boilers. Sylwester *et al.* [10] took the convective heating surface of a specific power plant boiler as the research object, through a large number of experiments, collected the ash deposition data, combined with the variables such as boiler structure, coal quality, flue gas flow rate, etc., established the ash deposition model, and applied the model to the boiler soot blowing optimization. Vassallo *et al.* [11] used Fourier transform infrared emission spectroscopy to study the deposition process of coal ash in a mini-type furnace. Peña *et al.* [12], Teruel *et al.* [13], and Lu *et al.* [14] used neural networks, fuzzy neural networks, and other intelligent algorithms to establish real-time monitoring models for heating surface fouling. The research above can monitor the state of the boiler on-line, give simple and optimized soot blowing guidance in different ways, and lay a good foundation for the monitoring of the heating surface of the boiler. The thermal power operation optimization software developed by many internationally renowned power generation equipment suppliers contains an ash pollution monitoring module to optimize the operation of the soot blower. The boiler heating surface pollution monitoring system installed at Unit 5 of the Kraitwerk Power Plant [15] in Germany relies on the existing data acquisition system (DAS) to collect various parameters online. According to the principle of thermal equilibrium, the actual heat transfer coefficient calculated is compared with the ideal heat transfer coefficient, the degree of contamination of the heating surface is analyzed, and the soot blower cleaning heating surface is guided, so as to realize the closed loop automatic control of the ash blower's start and stop, thus proving the practicability of the module. Also, the Sootblow Advisor expert system [16], developed by New York Gas Company and General Physics Corporation, and the OPTIMAX computing package, independently developed by ABB of Switzerland [17], etc are operating in some power plants. Due to commercial confidentiality, the specific technical details are rarely reported. Due to the complexity of the operation and combustion system of coal-fired power station boilers, the soot blowing operation and the current boiler operating conditions require a certain amount of preparation time. During the preparation process, the ash is still deposited, which causes more coal consumption. This is a common problem in coal-fired power station boilers. At the present stage, energy conservation and emission reduction put forward higher requirements for ash blowing optimization. If the ash fouling condition of the heating surface can be predicted and the soot blowing preparation is made ahead of time, the occurrence of untimely soot blowing can be avoided.

Given the general problem of dust injection in coal-fired utility boilers, a method for predicting the cleanliness of heating surfaces is proposed by analyzing the monitoring data of heating surfaces. In this method, the fouling rate (FF) is used as the monitoring index of the clean state of the heating surface of the coal-fired power plant boiler. Firstly, the historical fouling rate data is decomposed into two parts: fitting curve data and the difference between original data and the fitting curve. Secondly, the difference between the original data and the fitting curve (residual error) is analyzed, and the mathematical expectation is obtained. Thirdly, the real-time fouling rate data is fitted, combined with the difference expectation, the prediction model is established. Finally, the soot blowing operation is guided to optimize steam consumption and heat transfer efficiency. This method does not need additional special instruments and a complex calculation system and can use the existing monitoring data to realize the dirt monitoring and ash blowing optimization of the economizer. The method is verified by the actual operation data of a 300MW coal-fired power station boiler. By analyzing and comparing the prediction results of the future fouling state of the heating surface with the prediction model proposed in this paper and the Elman prediction model, it is found that the resulting error of the prediction model using the new method is smaller and has a good prediction accuracy. The new method is used to predict the future state of the heating surface and prepare the ash blowing operation in advance, which has a certain guiding role for the ash blowing operation of thermal power plants.

II. REASEARCH OBJECT

The research object of this manuscript is a boiler economizer for a 300MW unit of a coal-fired thermal power station. The main design parameters of the boiler are shown in Table 1.

TABLE 1. Main design parameters of the unit.

Parameter	Unit	Value of number
Rated condition	MW	300
Fuel flow	kg/s	35.4
Rated evaporation	t/h	909.6
Rated main steam pressure	MPa	17.25
Rated main steam temperature	^oC	540
Reheat steam flow	t/h	743.2
Reheat steam pressure	MPa	3.18
Reheat steam temperature	^oC	540
Feedwater temperature	^oC	278
Air volume	kg/s	295

III. PRINCIPLE OF SOOT ACCUMULATION MONITORING

In the calculation of the heating surface of the boiler unit, some parameters (thermal resistance of ash and dirt, cleaning

factor, etc.) that can represent the cleaning state of the heating surface are usually used to represent the cleaning state of the heating surface [18]. Generally, these parameters are the characteristic parameters that can be directly measured or observed during the normal operation of some boilers, which are obtained through mathematical modeling, that is, the ash monitoring process is the parameter modeling process that represents the ash pollution degree of the heating surface [19]. In this manuscript, the real-time monitoring data of the DCS system of a coal-fired power plant is combined with the basic thermodynamic calculation data needed for modeling. According to the dynamic energy balance theorem, the real-time monitoring model is established by mathematical modeling. The fouling degree of each heating surface is characterized by the fouling rate (FF) of each convection heating surface, dimensionless. The definition of the fouling rate is as follows:

$$FF = 1 - \frac{K_r}{K_t} \tag{1}$$

where K_r, K_t are the actual and theoretical heat transfer coefficients of the heating surface, dimensionless. When FF = 0, it means that the initial ash pollution state of the boiler heating surface is the most ideal clean state. The closer it is to 0, the less the ash pollution on the heating surface, the cleaner it is; when FF is greater than 0, it means that the heating surface is in a polluted state, and the closer it is to 1, the more serious the pollution on the heating surface of the boiler. As mentioned above, the fouling level of the heat transfer surface can be described by the fouling rate.

A. THEORETICAL HEAT TRANSFER COEFFICIENT

The theoretical heat transfer coefficient K_t indicates the efficiency of the heat transfer of the heating surface when the heating surface is clean. When neglecting the thermal resistance of the working substance and the tube wall and the thermal resistance inside the metal, the sum of the theoretical radiation heat transfer coefficient and the theoretical convection heat transfer coefficient is usually the sum of the theoretical heat transfer coefficient.

$$K_t = \alpha_f + \alpha_d \tag{2}$$

$$\alpha_{\mathrm{f}} = 5.7 \times 10^{-8} \frac{a_{gb}+1}{2} a_h T^3 \kappa \tag{3}$$

where α_f is the theoretical radiation heat transfer coefficient and α_d is the theoretical convection heat transfer coefficient.

The heat transfer coefficient of the heating surface is usually calculated by the following formula [20]:

$$\alpha_d = 0.65 C_s C_z \frac{\lambda}{d} \left(\frac{\omega d}{\upsilon}\right)^{0.64} \mathrm{Pr}^{\frac{1}{3}} \tag{4}$$

where

$$\kappa = \left\{ \left(1 - \left(\frac{T_{gb}}{T}\right)^4\right) \Big/ \left(1 - \frac{T_{gb}}{T}\right) \right\} \tag{5}$$

where a_{gb} is the blackness of the pipe wall;

a_h is the blackness of flue gas;

T is the temperature of flue gas in the metal pipe of economizer, $^\circ C$;

T_{gb} is the temperature of the outer wall of the metal pipe of the economizer, $^\circ C$;

C_s is the transverse structural parameter of the heating surface;

C_z is the transverse structural parameter of the heating surface;

λ is the thermal conductivity of flue gas (used to express the thermal conductivity of flue gas);

d is the diameter of the metal pipe wall of economizer, m;

ω is the flow velocity of flue gas inside the metal pipe of economizer, m/s;

υ is the dynamic viscosity of flue gas;

Pr is the Prandtl number.

The flue gas velocity can be obtained by the following formula:

$$\omega = \frac{V_b}{A} \tag{6}$$

where, A is the heat exchange area of the convective heating surface, m^2;

V_b is the flue gas flow through the convective heating surface under the standard condition, m^3/s, which can be obtained by measuring the actual flue gas flow V_r through the Clapeyron equation:

$$V_b = \frac{p_r V_r}{p_b} \Big/ \left(1 + \frac{T_r}{273.15}\right) \tag{7}$$

where, V_r is the actual measured flue gas flow, m^3/s;

T_r is the measured temperature of the flue gas, $^\circ C$;

p_r is the pressure of the flue gas, Pa;

p_b is the standard atmospheric pressure, Pa.

B. ACTUAL HEAT TRANSFER COEFFICIENT

The actual heat transfer coefficient of this manuscript is obtained by dynamic energy balance and iterative method [21]:

$$K_r = \frac{Q_y}{A \Delta t} \tag{8}$$

where Q_y is the heat released by the flue gas inside the metal pipe of the economizer, kJ/s;

A is the heat exchange area of the heating surface pipeline of the economizer, m^2;

Δt is the average value of the temperature difference between the flue gas side and the working medium side of the heat exchange surface, $^\circ C$, defined as:

$$\Delta t = (\Delta T_{\max} - \Delta T_{\min}) \Big/ \ln \frac{\Delta T_{\max}}{\Delta T_{\min}} \tag{9}$$

where $\Delta T_{\max}$ and $\Delta T_{\min}$ respectively represents the maximum and minimum temperature difference between the flue gas side and the working medium side of the heating surface, $^\circ C$ Calculate the dynamic heat release Q_y [15], including the following three parts: metal heat storage change ΔQ_{jx}, working medium heat storage change ΔQ_{gz}, and working

medium heat absorption Q_g, the three calculation formulas are as follows:

$$\Delta Q_{jx} = m_{jx} c_{jx} \frac{\partial t_{jx}}{\partial \tau} \tag{10}$$

$$\Delta Q_{gz} = m_{gz} c_{gz} \frac{\partial t_{gz}}{\partial \tau} \tag{11}$$

$$Q_g = D(H_{out} - H_{in}) \tag{12}$$

where m_{jx}, m_{gz} are respectively the mass of the metal tube wall of the heating surface and the working medium flowing through it, kg;

c_{jx}, c_{gz} are the average specific heat capacity of the metal tube wall of the heating surface and the working medium flowing through it respectively, $kJ/kg \cdot {}^\circ C$;

t_{jx} is the instantaneous temperature of the metal tube wall of the heating surface, ${}^\circ C$;

t_{gz} is the instantaneous temperature of the working medium flowing through the wall of the heating surface, ${}^\circ C$;

D is the working fluid flow through the heating surface, kJ/s;

H_{in} is the enthalpy value of working medium flowing through the heating surface, kJ/kg;

H_{out} is the enthalpy value of the working medium flowing through the outlet of the heating surface, kJ/kg;

τ is time, s.

IV. DATA PATA PREPROCESSING AND SELECTION

A. DATA PREPROCESSING

Data preprocessing is to eliminate outliers and smooth the collected data to ensure the accuracy of subsequent experiments.

1) The elimination of outliers is based on the method of laida (non-equal confidence probability). Its basic idea is: if the difference between a measured value and the average value is more than three times the standard deviation, it will be eliminated.

$$|x_1 - \bar{x}| > 3S_x \tag{13}$$

where $\bar{x} = \frac{1}{n}\sum_{i=1}^{n} x_i$ is the sample mean, $S_x = \left(\frac{1}{n}\sum_{i=1}^{n}(x_1 - \bar{X})^2\right)^{\frac{1}{2}}$ is the standard deviation of the sample.

2) The basic idea of the ''weighted moving average'' smoothing filtering method is used in data smoothing: the data weight at the center of the average interval is the largest, and the farther away from the center, the smaller the data weight.

$$\hat{y}_m = 0.025y_{m-3} + 0.05y_{m-2} + 0.075y_{m-1} + 0.7y_m + 0.075y_{m+1} + 0.05y_{m+2} + 0.025y_{m+3} \tag{14}$$

where $\hat{y}_m$ is the result after filtering; y_m is the actual measurement value at m time.

Taking a set of experimental data as an example, the effect of data preprocessing is illustrated. Fig 1 shows the original

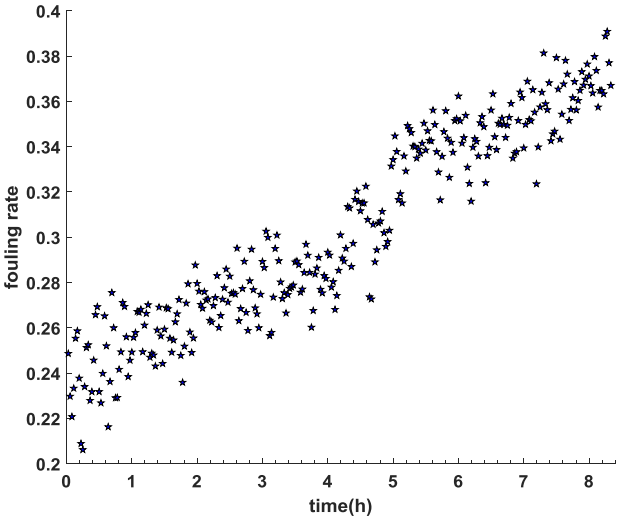

(a). data without preprocessing

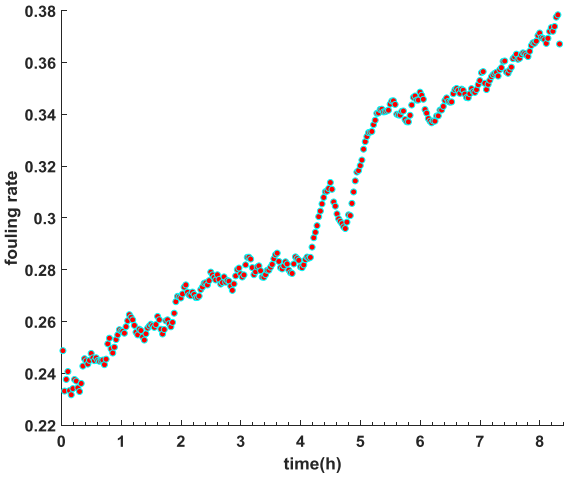

(b). data after preprocessing

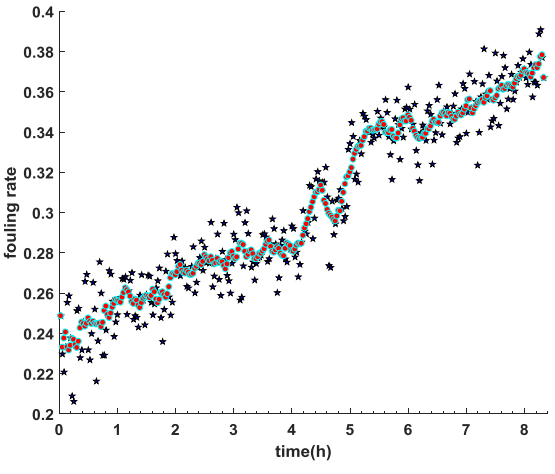

(c) data comparison before and after data preprocessing

FIGURE 1. Data preprocessing.

data in the DCS database and the results after data processing. By comparing the data before and after processing, it is found that the larger burr in the original data has been processed. After data preprocessing, the overall trend of the data has not changed. It can better analyze the trend of data changes.

B. DATA SELECTION

As shown in Fig. 2, the vertical axis on the left represents the fouling rate of the heating surface of the economizer, the vertical axis on the right represents the load, and the horizontal axis represents the time. "Soot blowing" represents the "soot blowing process of heating surface". The part between the two "soot blowing" represents the "ash deposition process of the heating surface". In the stage of stable load, the fouling rate has a more obvious change trend. In the process of soot blowing, the fouling rate of the heating surface decreases; on the contrary, in the process of soot deposition, the fouling rate of the heating surface increases. However, in the stage of rapid load change, the change of the fouling rate of the economizer is relatively chaotic. In the process of load stabilization, the changing trend of the fouling rate of the heating surface is consistent with the change of ash content of the heating surface, which is suitable for the change of heat transfer efficiency of reaction heating surface. However, the fluctuation of the fouling rate in the stage of load change is too large to reflect the actual heat transfer efficiency of the heating surface. Therefore, the data used in this manuscript is from the ash deposition process of the load stability stage.

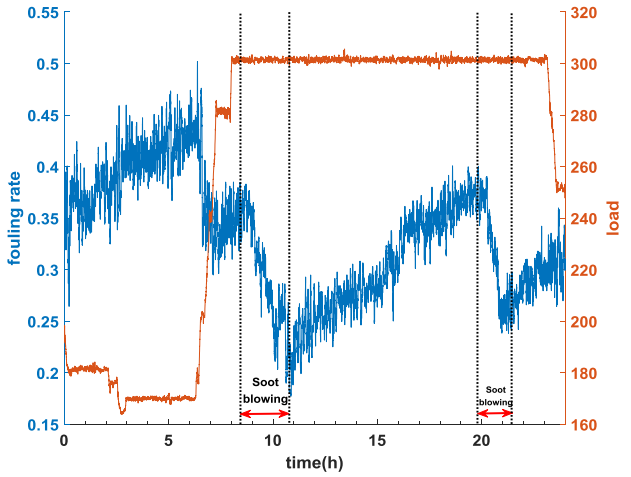

FIGURE 2. Curve of fouling rate of heating surface and load with time in 24 hours.

The bad point processing and data smoothing processing are carried out for the collected operation parameters of the boiler. Then the data collected in the boiler DCS system is calculated and analyzed with a sampling interval of 100s. The available data collected from the DCS system of the boiler are selected and 21 sets of available data are obtained. These 21 sets of data almost include all typical working conditions of the boiler under normal operating conditions. The 21 sets of data used in this manuscript have 300 points in each set. Randomly selected 18 sets of data in 21 sets of data as an experimental data set, as shown in Fig. 3(a), and the other three sets of data as the test data set, as shown in Fig. 3(b). In Fig. 3, the abscissa is the time, the unit is h, and the ordinate is the fouling rate.

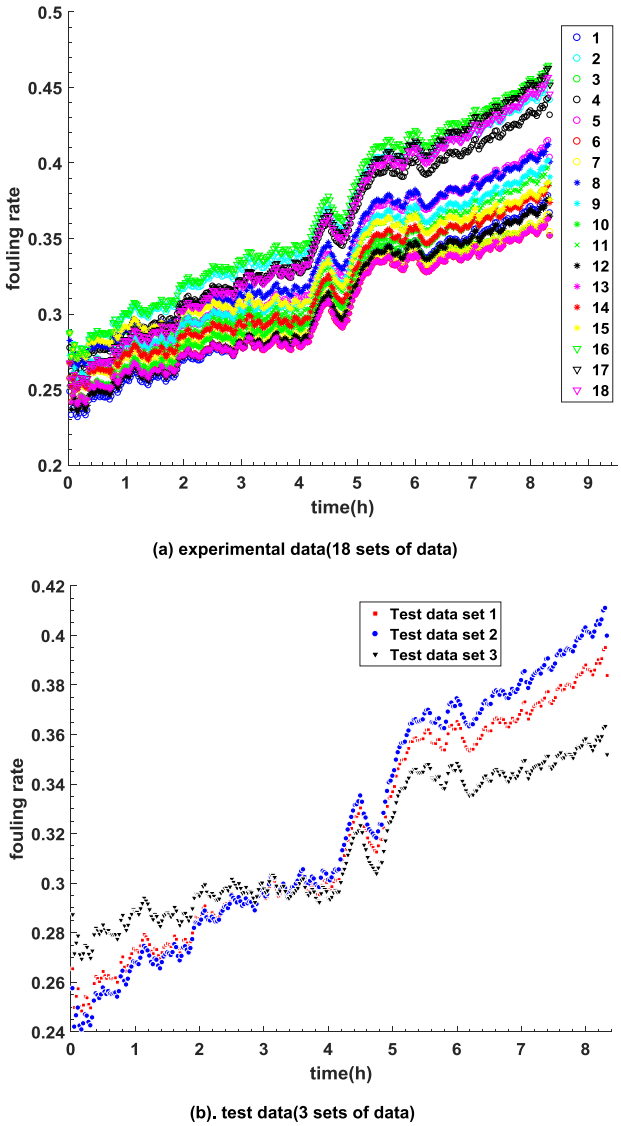

FIGURE 3. Fouling rate data of heating surface.

C. ESTABLISHMENT OF THE PREDICTION MODEL

Step 1: 18 sets of pre-processing fouling rate data were fitted.

Step 2: Decompose each set of data into two parts: the fitting curve, residual error(the difference between the original data and the fitting curve). Fig 4 shows the data after data decomposition, the vertical coordinate is the fouling rate; The horizontal coordinate is the time, and the formula under each figure is the formula of the fitting curve. Due to the

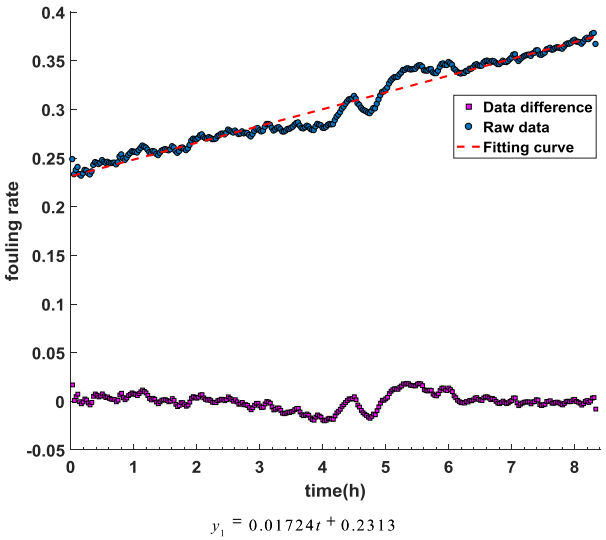

$y_1 = 0.01724t + 0.2313$

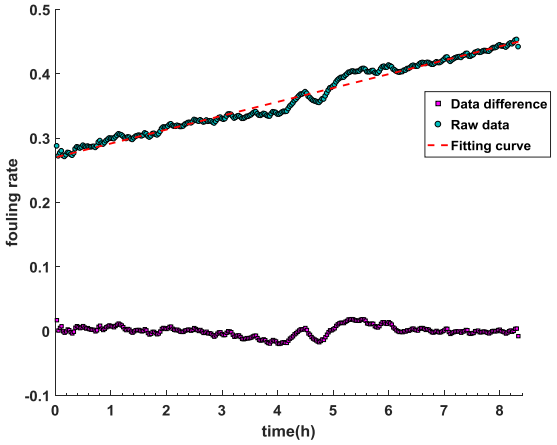

$y_2 = 0.02156t + 0.27$

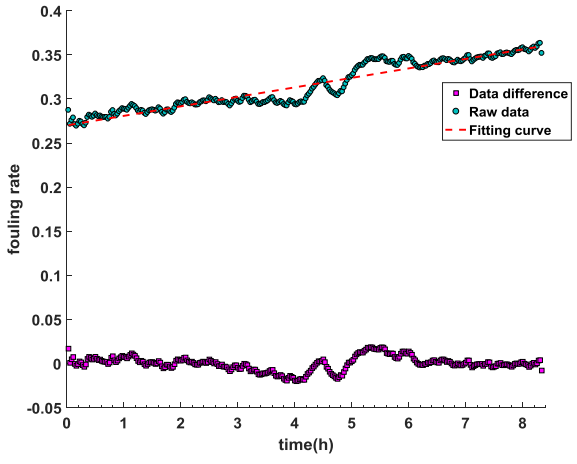

$y_3 = 0.01076t + 0.2710$

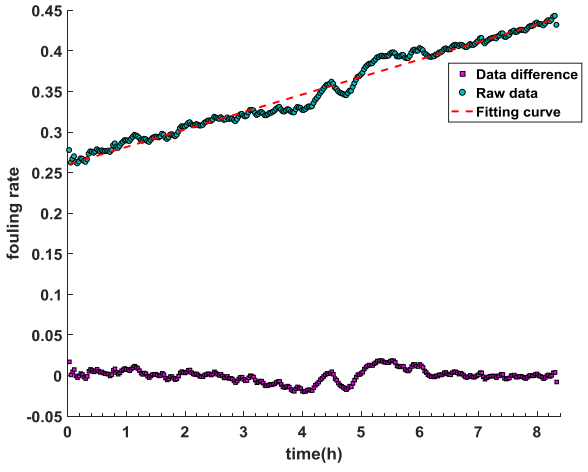

$y_4 = 0.02156t + 0.26$

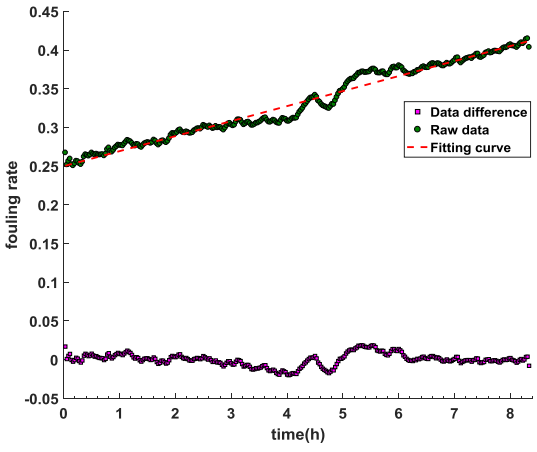

$y_5 = 0.0194t + 0.25$

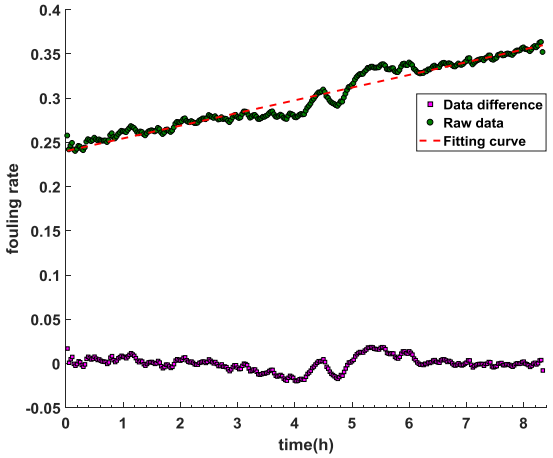

$y_6 = 0.01436t + 0.2401$

FIGURE 4. Decomposition of fouling rate data (6 sets of data in 18 groups).

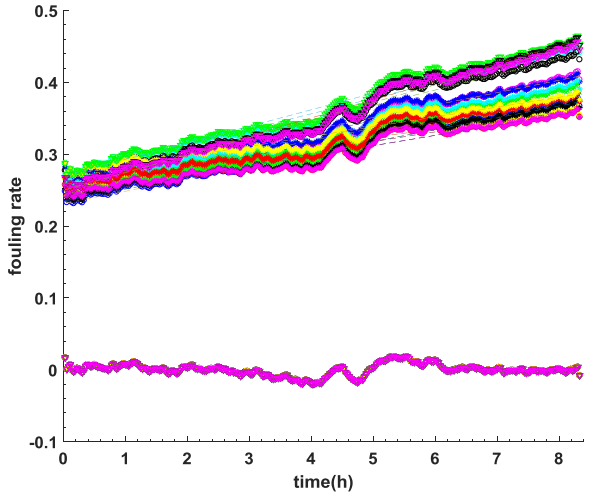

FIGURE 5. Decomposition of fouling rate data (the upper part of the figure is 18 sets of data and the corresponding fitting curve, and the lower part is the residual part).

limitation of the length of the manuscript, the decomposition diagram of 18 sets of experimental data is not put in the manuscript. Fig. 4 is only 6 sets of 18 sets of data. Fig. 5 is a full breakdown of 18 sets of data, including the original data, fitting curve, and residual error (date difference).

Step 3: After 18 sets of data are decomposed, residual error (date difference) and the fitting curve is integrated to get Fig. 6. From Fig. 6, it can be seen that residual error and the fitting curve of 18 sets of data are very close. The difference between 18 sets of original data and the fitting curve is used to solve the mathematical expectation. As shown in Fig. 7, the corresponding part of ''average'' is called the residual expectation.

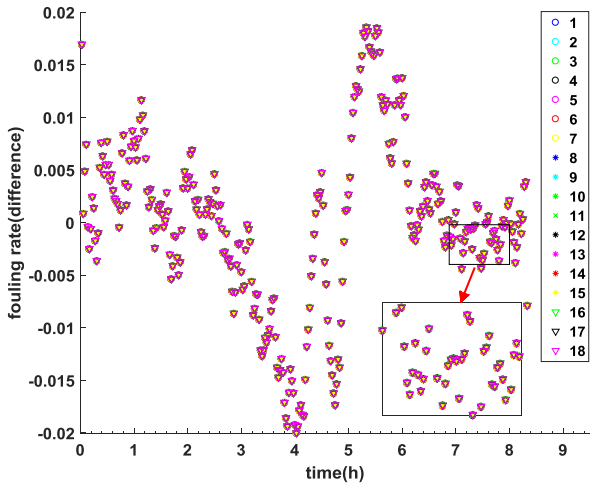

FIGURE 6. Residual error of 18 sets of fouling rate data.

Step 4: Firstly, the first N points of 300-time points in the validation data set are fitted to get the fitting curve $y = at + b$ (where a and b are fitting parameters respectively). Then, the time point (i.e. the abscissa corresponding to 300-N) of the part without data fitting is brought into the

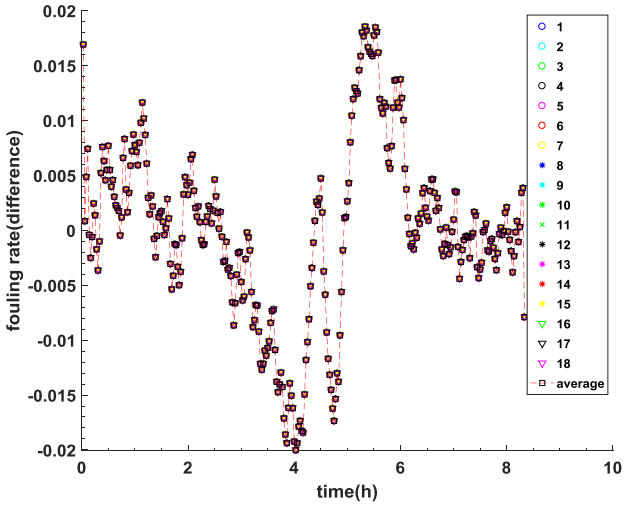

FIGURE 7. Residual error and expectation of 18 sets of data.

fitting curve $y = at + b$, and the resulting value is called ''fitting value''. Finally, the fitting value of 300-N time points behind the validation data, and the expectation of residual error is added in turn to get the prediction value, which is called the ''residual expectation method''.

V. EVALUATING INDICATOR

To compare the prediction accuracy of the two methods, MSE (mean squared error) and MAE (mean absolute error) are used as evaluation criteria.

A. MEAN SQUARED ERROR

Mean square error refers to the expected value of the square of the difference between the estimated value of the parameter and the true value of the parameter. MSE can evaluate the degree of change of the data. The smaller the value of MSE is, the better the accuracy of the prediction model to describe the experimental data is. The calculation formula is as follows:

$$MSE = \frac{1}{m}\sum_{i=1}^{m}(y_i - \hat{y})^2 \tag{15}$$

where y_i is the true value of the sample; $\hat{y}$ is the predicted value.

B. MEAN ABSOLUTE ERROR

The mean absolute error is the mean value of the absolute error, which can better reflect the actual situation of the predicted value error. The calculation formula is as follows:

$$MAE = \frac{1}{m}\sum_{i=1}^{m}\left|(y_i - \hat{y}_i)\right| \tag{16}$$

VI. EXPERIMENTAL VERIFICATION

When N = 250, 200, and 150, the predicted values can be obtained respectively by using the residual expectation method proposed in this manuscript. Besides, by using Elman neural network, the fouling rates corresponding to the first

250, 200, and 150-time points of 300-time points are trained as training sets, and the fouling rate corresponding to the next 50, 100 and 150-time points are tested as test sets.

A. WHEN N=250

The fitting curve of the first 250 time points in test data set 1 is $y = 0.01742t + 0.2476$. The comparison between Elman neural network and residual expectation method is as follows:

The fitting curve of the first 250 time points in test data set 2 is $y = 0.02029t + 0.2396$. The comparison between Elman neural network and residual expectation method is as follows:

The fitting curve of the first 250 time points in test data set 3 is $y = 0.01094t + 0.2697$. The comparison between Elman neural network and the new method is as follows:

As shown in Figs.8-10 and Tables 2-4, when N=250, compared with the Elman neural network method, the test data set 1, 2, and 3 adopt residual expectation method to predict the pollution of the heating surface more accurately.

TABLE 2. N = 250, comparison of prediction accuracy (Test data set 1).

Method	MSE	MAE
Elman neural network prediction	9.8×10^{-5}	9.200×10^{-3}
New method forecast	8.7819×10^{-7}	9.3487×10^{-4}

TABLE 3. N = 250, comparison of prediction accuracy (Test data set 2).

Method	MSE	MAE
Elman neural network prediction	5.646×10^{-5}	6.339×10^{-3}
New method forecast	8.125×10^{-7}	8.990×10^{-4}

TABLE 4. N = 250, comparison of prediction accuracy (Test data set 3).

Method	MSE	MAE
Elman neural network prediction	3.040×10^{-5}	4.738×10^{-3}
New method forecast	8.963×10^{-7}	9.440×10^{-4}

B. WHEN N=200

The fitting curve of the first 200 time points in test data set 1 is $y = 0.01626t + 0.2498$. The comparison between Elman neural network and the new method is as follows:

The fitting curve of the first 200 time points in test data set 2 is $y = 0.01913t + 0.2418$. The comparison between Elman neural network and residual expectation method is as follows:

The fitting curve of the first 200 time points in test data set 3 is $y = 0.009777t + 0.2719$. The comparison between Elman neural network and residual expectation method is as follows:

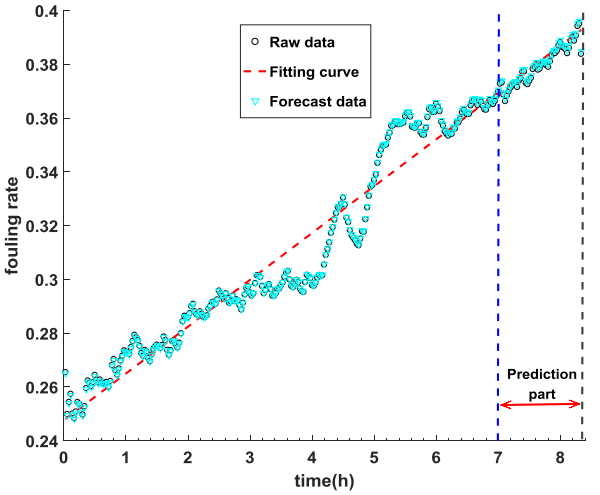

(a). prediction results of residual expectation method(test date set1)

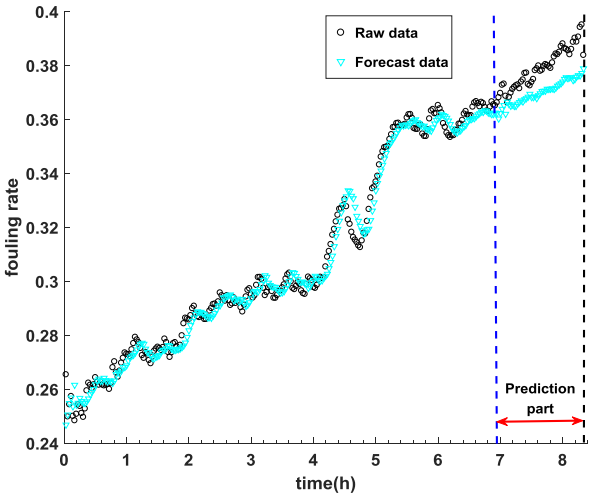

(b). prediction results of Elman neural network(test date set 1)

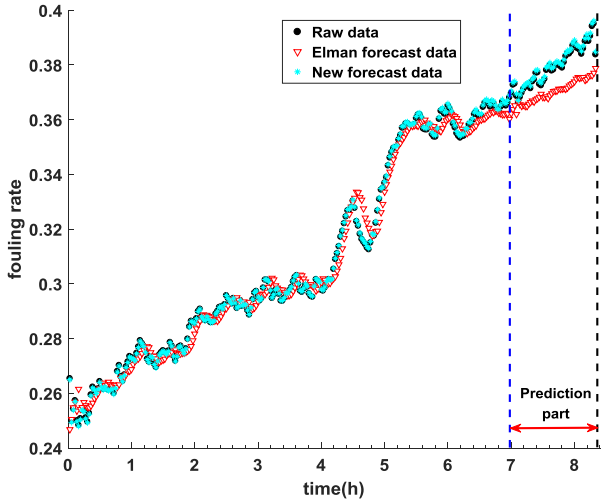

FIGURE 8. N = 250, comparison of two prediction methods (Test data set 1).

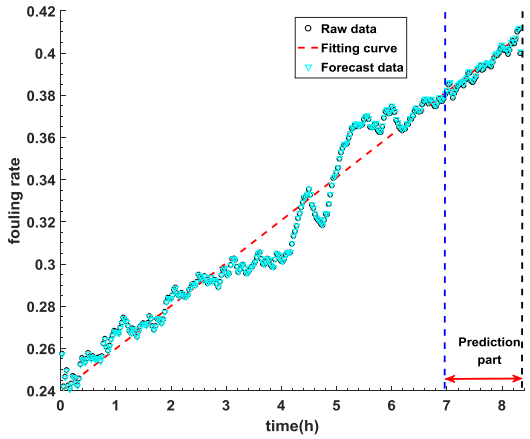

(a). prediction results of residual expectation method(test date set 2)

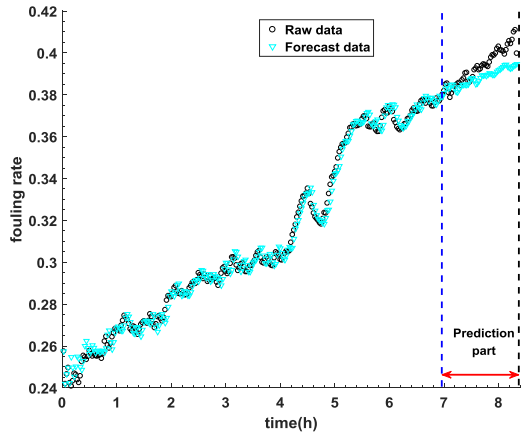

(b). prediction results of Elman neural network(test date set 2)

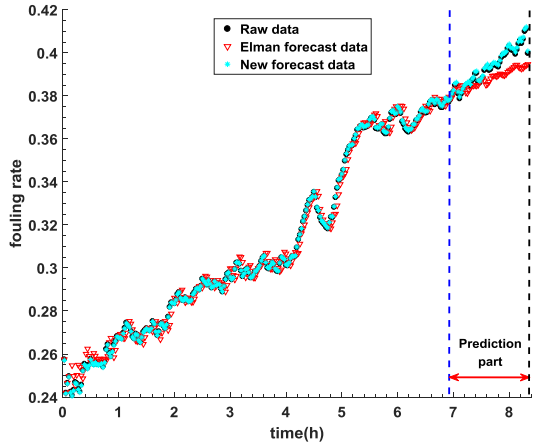

FIGURE 9. N = 250, comparison of two prediction methods (Test data set 2).

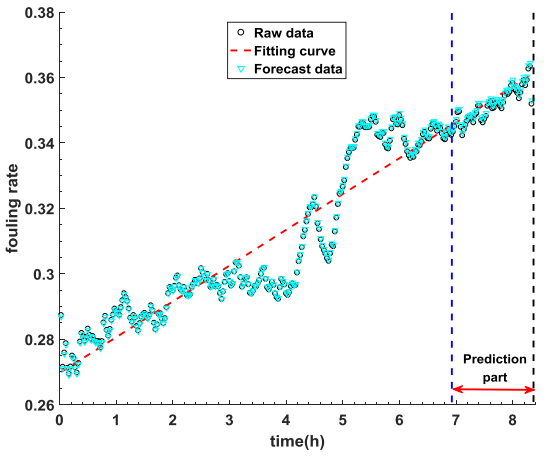

(a). prediction results of residual expectation method(test date set 3)

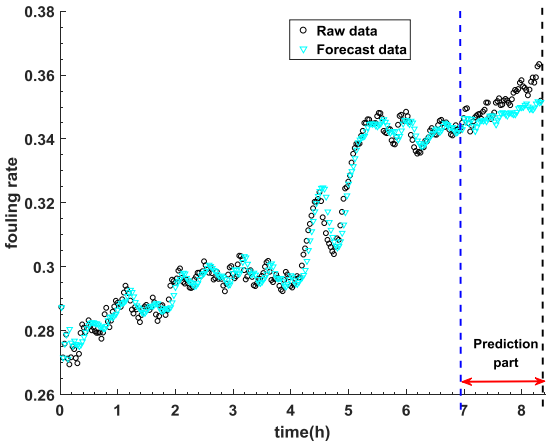

(b). prediction results of Elman neural network(test date set 3)

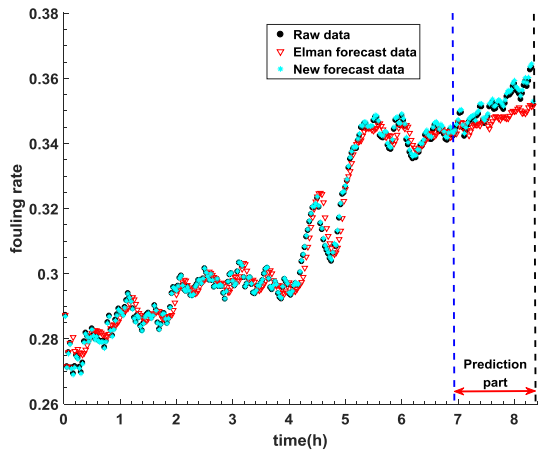

FIGURE 10. N = 250, comparison of two prediction methods (Test data set 3).

As shown in Figs. 11-13 and Tables 4-7, when N=200, compared with the Elman neural network, residual expectation method is more accurate in predicting the pollution of heating surface in test data sets 1, 2, and 3. However, compared with the two prediction methods when N=250, the prediction accuracy of the Elman neural network and residual expectation method for heating surface pollution has a certain decline.

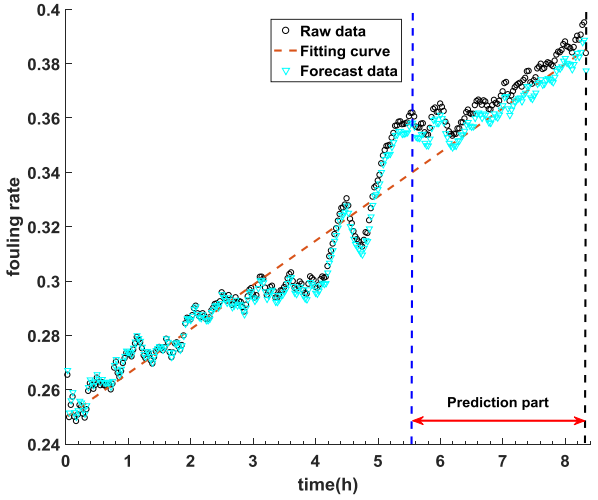

(a). prediction results of residual expectation method(test date set1)

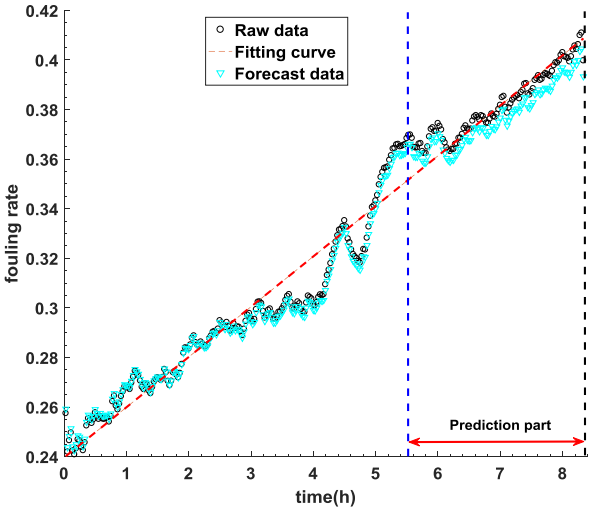

(a). prediction results of residual expectation method(test date set 2)

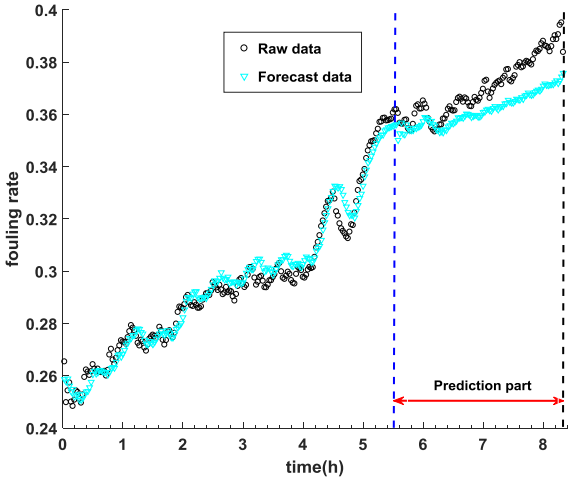

(b). prediction results of Elman neural network(test date set 1)

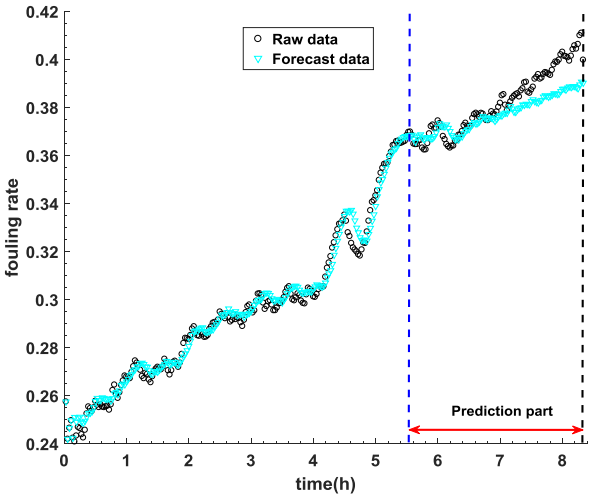

(b). prediction results of Elman neural network(test date set 2)

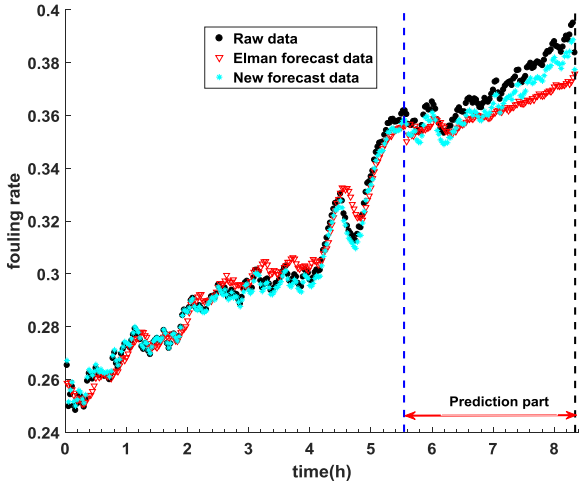

FIGURE 11. N = 200, comparison of two prediction methods (Test data set 1).

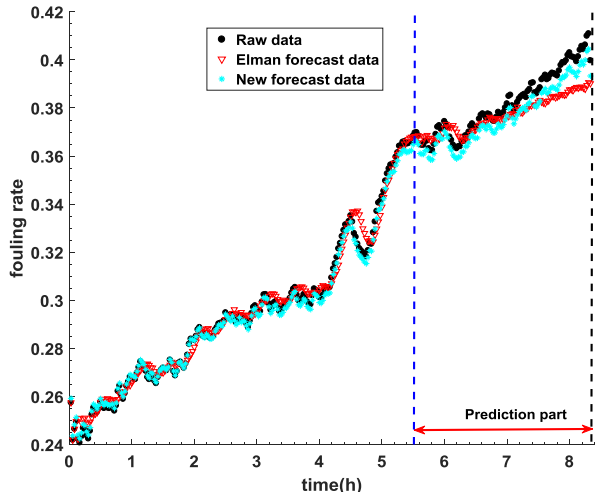

FIGURE 12. N = 200, comparison of two prediction methods (Test data set 2).

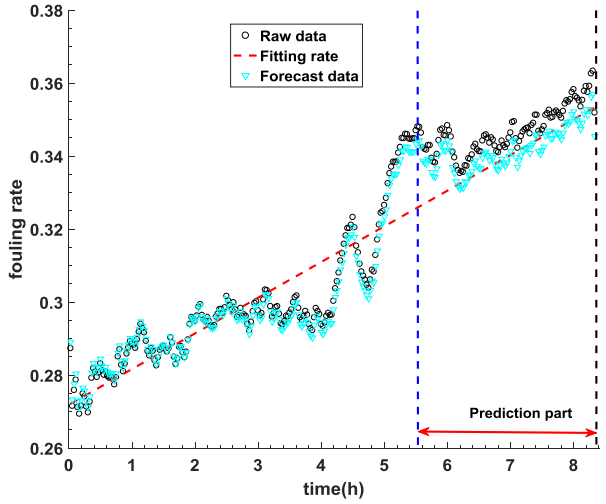

(a). prediction results of residual expectation method(test date set 3)

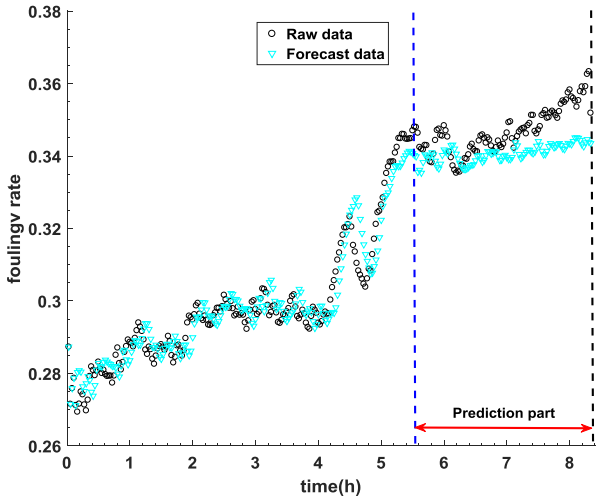

(b). prediction results of Elman neural network(test date set 3)

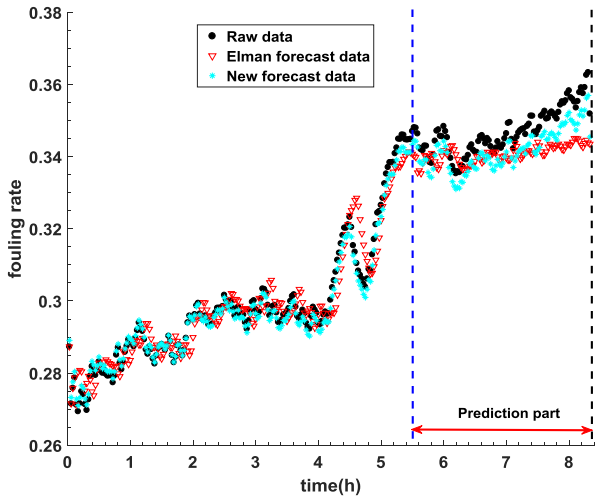

FIGURE 13. N = 200, comparison of two prediction methods (Test data set 3).

TABLE 5. N = 200, comparison of prediction accuracy (Test data set 1).

Method	MSE	MAE
Elman neural network prediction	9.700×10^{-5}	8.500×10^{-3}
New method forecast	2.624×10^{-5}	5.100×10^{-3}

TABLE 6. N = 200, comparison of prediction accuracy (Test data set 2).

Method	MSE	MAE
Elman neural network prediction	6.719×10^{-5}	6.474×10^{-3}
New method forecast	2.655×10^{-5}	5.091×10^{-3}

TABLE 7. N = 200, comparison of prediction accuracy (Test data set 3).

Method	MSE	MAE
Elman neural network prediction	6.548×10^{-5}	6.782×10^{-3}
New method forecast	2.636×10^{-5}	5.073×10^{-3}

C. WHEN N=150

The fitting curve of the first 150 time points in test data set 1 is $y = 0.01207t + 0.2569$. The comparison between Elman neural network and residual expectation method is as follows:

The fitting curve of the first 150 time points in test data set 2 is $y = 0.01495t + 0.2489$. The comparison between Elman neural network and residual expectation method is as follows:

The fitting curve of the first 150 time points in test data set 3 is $y = 0.005592t + 0.2790$. The comparison between Elman neural network and residual expectation method is as follows:

It can be seen from Figs. 14-16 and Tables 8-10 that when N=150, the prediction accuracy of Elman neural network and residual expectation method for heating surface pollution of test data 1, 2, and 3 are very poor.

TABLE 8. N = 150, comparison of prediction accuracy (Test data set 1).

Method	MSE	MAE
Elman neural network prediction	4.0333×10^{-4}	0.0190
New method forecast	5.92×10^{-4}	0.0235

TABLE 9. N = 150, comparison of prediction accuracy (Test data set 2).

Method	MSE	MAE
Elman neural network prediction	9.890×10^{-4}	2.852×10^{-2}
New method forecast	5.900×10^{-4}	2.486×10^{-2}

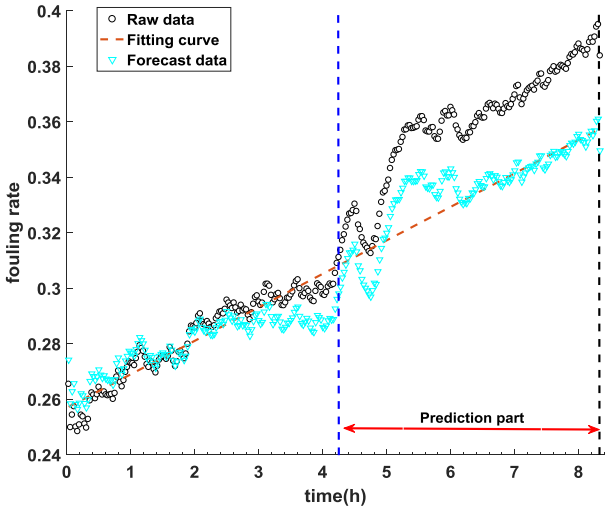

(a). prediction results of residual expectation method(test date set 1)

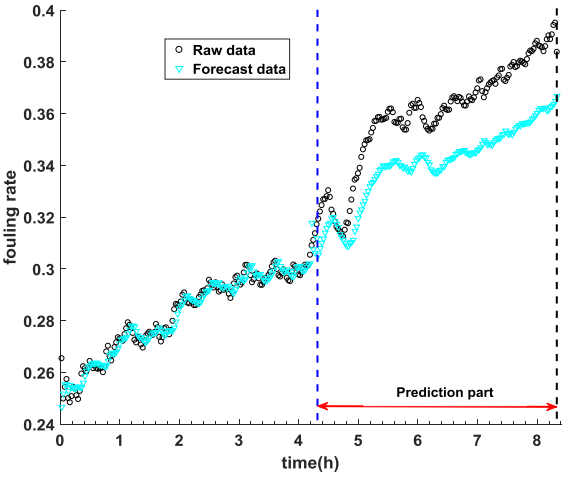

(b). prediction results of Elman neural network(test date set 1)

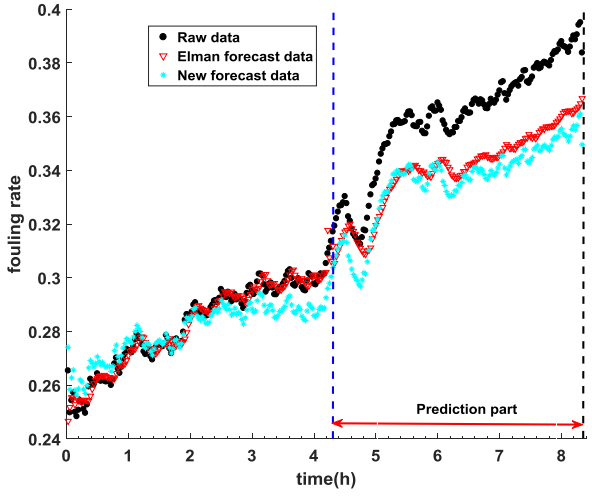

FIGURE 14. N = 150, comparison of two prediction methods (Test data set 1).

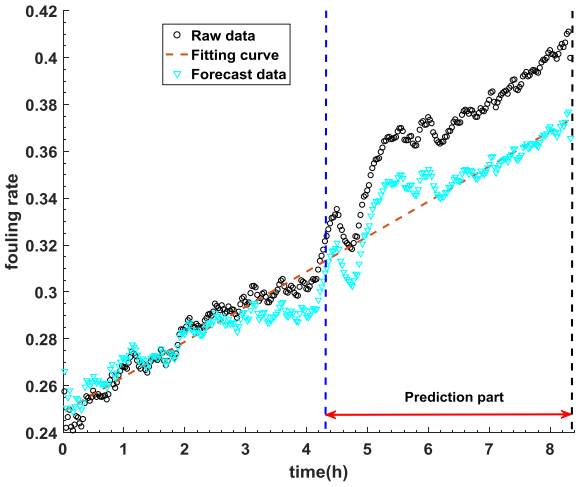

(a). prediction results of residual expectation method(test date set 2)

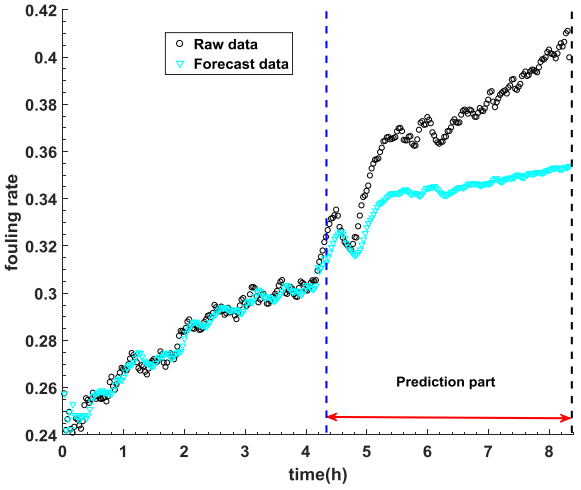

(b). prediction results of Elman neural network(test date set 2)

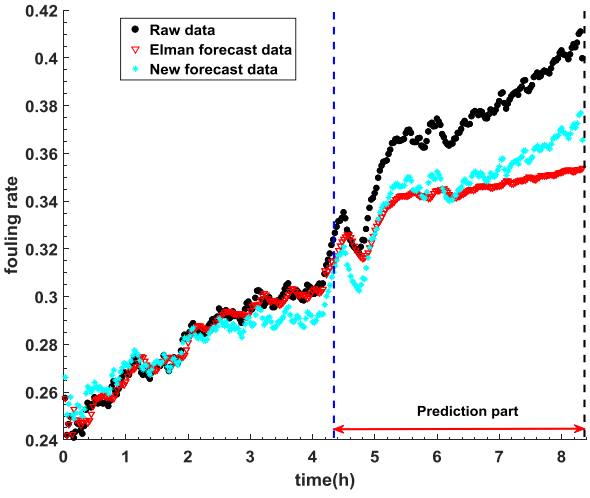

FIGURE 15. N = 150, comparison of two prediction methods (Test data set 2).

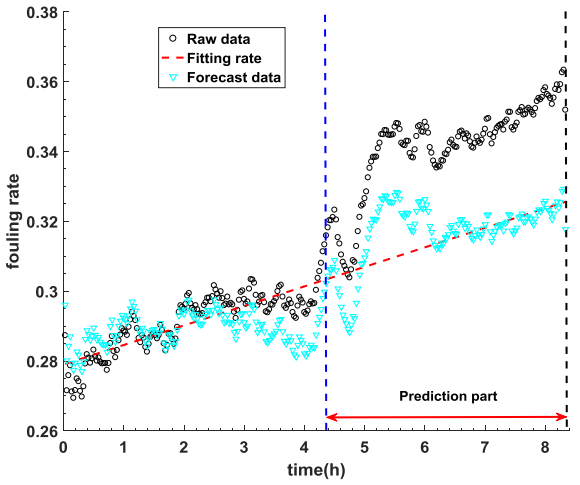

(a). prediction results of residual expectation method(test date set 3)

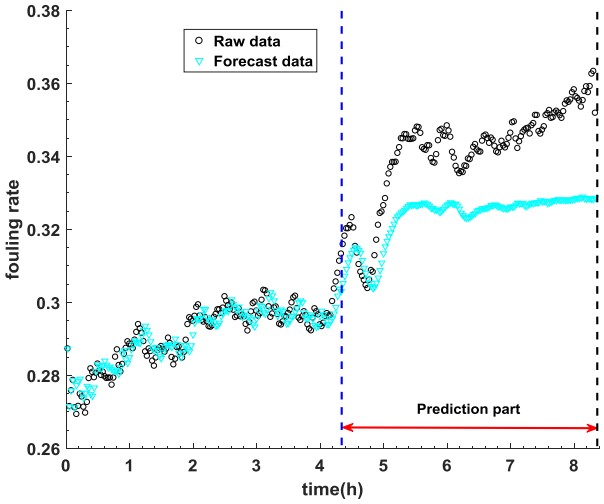

(b). prediction results of Elman neural network(test date set 3)

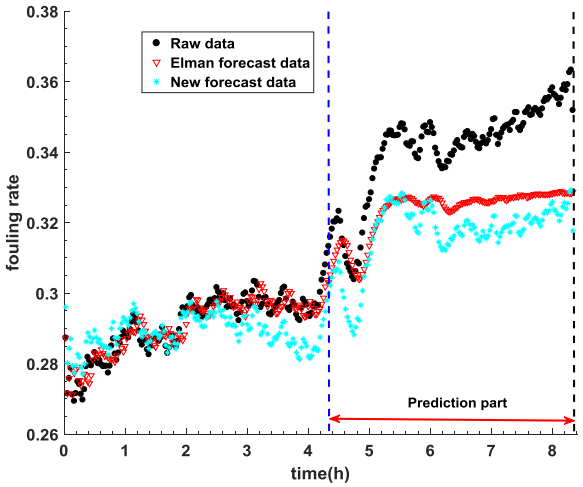

FIGURE 16. N = 150, comparison of two prediction methods (Test data set 3).

TABLE 10. N = 150, comparison of prediction accuracy (Test data set 3).

Method	MSE	MAE
Elman neural network prediction	3.610×10^{-4}	1.775×10^{-2}
New method forecast	5.910×10^{-4}	2.350×10^{-2}

D. RESULT ANALYSIS

By comparing the residual expectation method with Elman neural network (Figs. 8-16), it is found that when N=250 and 200, the new method has higher prediction accuracy than Elman neural network. When N=150, the prediction accuracy of both methods is very poor. Compared with the new method, Elman neural network prediction is more accurate, and they have no guiding significance for soot blowing on the heating surface. The time threshold of 300-time points of the experimental set data is [0, 8.33], that is, when N=250 and 200, the predictable time range is [6.94, 8.33] and [5.55, 8.33], respectively, and the time length is 1.39h and 2.78h. According to reference[18], when the soot deposition time is 7.62h (i.e. the fouling rate of heating surface reaches 0.36), the soot blowing starts. Assuming that the preparation time of soot blowing operation is T_r h, at (7.62-T_r)h, on the one hand, the power station staff starts to prepare for soot blowing operation; On the other hand, through the new method proposed in this manuscript, the real-time monitoring data of fouling rate from the end of the lastest soot blowing to (7.62-T_r)h is used to predict the soot pollution status of the heating surface in the future. When the fouling rate of the heating surface reaches 0.36, soot blowing starts. Under normal circumstances, the preparation time of soot blowing operation is generally about 0.5h, i.e. $T_r = 0.5h$. Therefore, using the real-time monitoring data of the scaling rate in the time from the end of the latest soot blowing operation to 7.12h, the dust pollution status of the heating surface is predicted. When N=250 and 200, the predicted time ranges are [6.94, 8.33] and [5.55, 8.33], respectively. The prediction accuracy of the fouling rate of the heating surface is very high. The prediction time (7.12h) is within these two-time ranges, so the new method can have a good prediction for the future state of ash pollution.

The actual operation data extracted in this paper has a time length of 8.33 h and a time range of [0, 8.33]. In this paper, the residual expectation method and Elman prediction model are used to predict the heating surface state of [6.94, 8.33]h respectively with [0, 6.94]h as training part, and [5.55, 8.33]h with [0, 4.16]h as training part, and [4.16, 8.33]h with [0, 4.16]h as training part. It is found that the prediction accuracy of the two methods is too poor for [0, 4.16]h as the training part and has no practical significance. The prediction results of the residual expectation method and Elman prediction model are analyzed and compared. It is found that the prediction model of the residual expectation method has a smaller error and has good prediction accuracy and feasibility.

VII. CONCLUSION

In this paper, safety, energy-saving, improve the overall operational efficiency and stability of coal-fired power plant boiler as the goal, aiming at some problems existing in the combustion process of the coal-fired power plant, taking the economizer as the research object, carried out the research work. In the first part of this paper, based on the on-line monitoring data and key parameters of the boiler economizer heating surface in the combustion process, the concept of fouling rate is used to reflect the ash pollution status of the heating surface, and a fouling monitoring model of the heating surface is established to facilitate on-line monitoring of the heat exchange efficiency of the economizer. In the second part of this paper, the real-time monitoring data of the economizer heating surface fouling rate are selected and preprocessed. Soot blowing operation is generally carried out under the condition of stable load, so the fouling rate data under the condition of too fast load change is not the research part of this paper. The research data selected in this paper is under a stable load condition. In the third part of this paper, by analyzing the existing data of the fouling rate of heating surface, a prediction method of fouling state of the heating surface is proposed, which can provide sufficient preparation time for soot blowing operation. The time range of fouling rate data selected in this paper is from the end of the last soot blowing operation as the starting point to the end of the next soot blowing operation as the endpoint, with a time length of 8.33 h, a total of 21 groups of data. Firstly, each group of data is fitted and decomposed into two parts, namely fitting part and residual (difference part of data and fitting part); then 18 groups of 21 groups of data are selected as training data set. By analyzing the residual parts of 18 groups of data sets, it is found that the residual parts of each group are very similar. The expectation of eighteen groups of data residuals was calculated. Finally, any three groups of 21 groups of data are selected as the experimental data set, and the data of the first half of each group of data are selected for fitting, and the fitting part is superimposed with the residual expectation to obtain the prediction model of fouling state of heating surface. This method does not need any calculation system and professional instruments, and can accurately predict the future state of the heating surface according to the real-time ash pollution data of the heating surface. The method proposed in this paper only needs to modify the monitoring of the heating surface and can be applied to other heating surfaces of boilers.

The next work of this paper is as follows:

1. Establish a soot blowing operation system based on the heating surface of different parts of the boiler (the area requiring soot blowing);

2. The existing soot blowing optimization models are all based on the premise of constant soot blowing steam pressure and flow, but the deposition rate and characteristics of soot fouling are different in different periods. On the premise of variable steam pressure and variable steam flow, it will also be one of the tasks to establish an optimization model for soot blowing.

ACKNOWLEDGMENT

The authors would like to thank the anonymous reviewers for their valuable suggestions to refine this work.

REFERENCES

[1] *Ministry of Planning and Development of China Electricity Union*, National Electric Power Industry Statistical Express Data List, 2018.

[2] A. Valero and C. Cortes, "Ash fouling in coal-fired utility boilers. Monitoring and optimization of on-load cleaning," *Prog. Energy Combustion Sci.*, vol. 22, no. 2, pp. 189–200, 1996.

[3] L. M. Romeo and R. Gareta, "Neural network for evaluating boiler Behaviour," *Appl. Thermal Eng.*, vol. 26, nos. 14–15, pp. 1530–1536, Oct. 2006.

[4] S. Aliakbari, M. Ayati, J. H. S. Osman, and Y. Md Sam, "Second-order sliding mode fault-tolerant control of heat recovery steam generator boiler in combined cycle power plants," *Appl. Thermal Eng.*, vol. 50, no. 1, pp. 1326–1338, Jan. 2013.

[5] Y. Han, C. Xu, G. Xu, Y. Zhang, and Y. Yang, "An improved flexible solar thermal energy integration process for enhancing the coal-based energy efficiency and NOx removal effectiveness in coal-fired power plants under different load conditions," *Energies*, vol. 10, no. 10, p. 1485, Sep. 2017.

[6] A. K. Sivathanu and S. Subramanian, "Extended Kalman filter for fouling detection in thermal power plant reheater," *Control Eng. Pract.*, vol. 73, pp. 91–99, Apr. 2018.

[7] J. Sandberg, R. B. Fdhila, E. Dahlquist, and A. Avelin, "Dynamic simulation of fouling in a circulating fluidized biomass-fired boiler," *Appl. Energy*, vol. 88, no. 5, pp. 1813–1824, May 2011.

[8] M. Dong, J. Han, S. Li, and H. Pu, "A dynamic model for the normal impact of fly ash particle with a planar surface," *Energies*, vol. 6, no. 8, pp. 4288–4307, 2013.

[9] Y. Shao, J. Wang, F. Preto, J. Zhu, and C. Xu, "Ash deposition in biomass combustion or co-firing for power/heat generation," *Energies*, vol. 5, no. 12, pp. 5171–5189, Dec. 2012.

[10] S. Kalisz and M. Pronobis, "Investigations on fouling rate in convective bundles of coal-fired boilers in relation to optimization of sootblower operation," *Fuel*, vol. 84, nos. 7–8, pp. 927–937, May 2005.

[11] A. M. Vassallo, P. A. Cole-Clarke, L. S. K. Pang, and A. J. Palmisano, "Infrared emission spectroscopy of coal minerals and their thermal transformations," *Appl. Spectrosc.*, vol. 46, no. 1, pp. 73–78, Jan. 1992.

[12] B. Peña, E. Teruel, and L. I. Díez, "Soft-computing models for soot-blowing optimization in coal-fired utility boilers," *Appl. Soft Comput.*, vol. 11, no. 2, pp. 1657–1668, Mar. 2011.

[13] E. Teruel, C. Cortés, L. Ignacio Díez, and I. Arauzo, "Monitoring and prediction of fouling in coal-fired utility boilers using neural networks," *Chem. Eng. Sci.*, vol. 60, no. 18, pp. 5035–5048, Sep. 2005.

[14] L. Jidong, L. Dingpo, L. Gang, and S. Kai, "Research on fuzzy model for the soot blowing optimization in utility boilers," *J. Huazhong Univ. Sci. Technol.*, vol. 33, no. 6, pp. 35–37, 2005.

[15] S. Zhang, G. Shen, L. An, and G. Li, "Ash fouling monitoring based on acoustic pyrometry in boiler furnaces," *Appl. Thermal Eng.*, vol. 84, pp. 74–81, Jun. 2015.

[16] S. Thompson and N. Li, "Boiler fouling, monitoring and control," *Computing Control Eng. J.*, vol. 3, no. 6, pp. 282–286, Nov. 1992.

[17] Y.-D. Zhu and Z.-Y. Gao, "The study on soot-blowing optimization based on theory of specific entropy generation," in *Proc. Asia–Pacific Power Energy Eng. Conf.*, Mar. 2009, pp. 1–5.

[18] Shi, Li, Wen, Cui, Pang, Jia, Zeng, and Wang, "Soot blowing optimization for frequency in economizers to improve boiler performance in coal-fired power plant," *Energies*, vol. 12, no. 15, p. 2901, Jul. 2019.

[19] Y. Shi, J. Wang, B. Wang, and Y. Zhang, "Real-time online monitoring of thermal efficiency in coal-fired power plant boiler based on coal heating value identification," *Int. J. Modelling Identificat. Control*, vol. 20, no. 3, pp. 295–304, 2013.

[20] Q. Fan and W. Yan, *Boiler Principles*. Beijing, China: China Electric Power Press, 2007.

[21] Y. Shi, J. Wang, and Z. Liu, "On-line monitoring of ash fouling and soot-blowing optimization for convective heat exchanger in coal-fired power plant boiler," *Appl. Thermal Eng.*, vol. 78, pp. 39–50, Mar. 2015.